Cocrystallization and Phase Segregation in Crystalline/Crystalline Polymer Blends of Bacterial Copolyesters

Naoko Yoshie,*,† Akeshi Asaka,‡ and Yoshio Inoue‡

Institute of Industrial Science, The University of Tokyo, Komaba, Meguro-ku, Tokyo 153-8505, Japan, and Department of Biomolecular Engineering, Tokyo Institute of Technology, 4259 Nagatsuta, Midori-ku, Yokohama 226-8501, Japan

Received January 20, 2004; Revised Manuscript Received March 9, 2004

ABSTRACT: Cocrystallization and phase segregation in blends of poly(3-hydroxybutyrate-*co*-3-hydroxyvalerate) [PHBV] and poly(3-hydroxybutyrate-*co*-3-hydroxypropionate) [PHBP] at 80−100 °C were analyzed through the in situ observation of crystallization by FTIR microscopy and the measurement of melting curve by DSC. To trace the crystallization process of the blend components separately by a FTIR microscope, deuterated PHBV (D-PHBV) is blended with normal PHBP. The C−D and C═O stretching bands of the IR spectra are used to trace the crystallization of D-PHBV and the whole blend, respectively. Five pairs of PHBV and PHBP were selected so as to make variations in the spherulite growth rates (G) of components and their difference. Three of them are the pairs of which PHBV has a higher G than PHBP. They show four types of crystalline phase structures with various extent of phase segregation: complete cocrystallization, cocrystallization forming PHBV-rich cocrystals, phase segregation forming PHBV-rich cocrystals and PHBP microcrystals, and phase segregation forming PHBV crystals and PHBP microcrystals. The extent of phase segregation depends on the G values and their difference. The lower G and the larger difference favor phase segregation. The other two blends are comprised of PHBP with a higher G value and PHBV with a lower G. Even if the G values and their difference fall within the range where the former three blends shows advanced phase segregation, the latter two blends show cocrystallization. This contradiction indicates another important factor, the compatibility of the monomers to the crystalline lattice of the other. PHBV shows isomorphous behavior; i.e., HV units can be partially included into the PHB lattice, while PHBP cannot. Therefore, any part of PHBV chains easily gets into these lamellas because the HV units in the chains can participate in the PHB-type crystalline lattice induced by PHBP. On the other hand, only the homogeneous sequences of HB units of PHBP can participate in the lamellas induced by PHBV.

Introduction

Cocrystallization of different polymers in polymer blends is a very rare phenomenon. The necessary conditions for cocrystallization of two different polymers are thought to be miscibility in the melt, similarity in the molecular structures, similarity in the crystalline lattice structures, and similarity in the crystallization rates. The second and third conditions are requirement for thermodynamic stability of cocrystals, while the first and forth conditions are for kinetic accessibility to form cocrystals. The thermodynamic requirements are quite tough. Additionally, even if the similarity in the structures ensures the cocrystallization in the equilibrium state, immiscibility and difference in the crystallization rate between the component polymers preclude the crystallization at the same time and at the same place. Cocrystallization has been observed only for a few blends of polymers, including blends of polyethylenes,[1,2] fluorocarbon polymers,[3−5] poly(aryl ether ketone)s,[6,7] and poly(3-alkylthiophene)s.[8] We have reported on the cocrystallization in the blends of poly(3-hydroxyalkanoate)s [PHAs].[9−13]

PHAs have attract much attention as biodegradable and biocompatible thermoplastic produced from renewable resources by bacterial fermentation.[14,15] Many studies on the physical, mechanical, and degradable properties, as well as structural characteristics, have been performed. Among them are the characterization of the blends of PHAs such as two poly(3-hydroxybutyrate-*co*-3-hydroxyvalerate)s [PHBVs][9−11,16−18] and two poly(3-hydroxybutyrate-*co*-3-hydroxypropionate)s [PHBPs][13] with different comonomer compositions. These blends provide a wide variety of phase structures from cocrystallization to immiscible phase separation, which can be controlled by careful selection of the sample preparation conditions and the difference, D_c, in the comonomer composition between the blend components. For the case of the blends of PHBVs, the blends show complete cocrystallization when D_c is less than ca. 10 mol %. Here, the complete cocrystallization indicates the crystallization forming crystals whose composition is the same as the whole blend. When D_c exceeds this level, the component of slower crystallization is partially excluded from the crystals. The content of this component in the cocrystals decreases with D_c, and finally, this component forms separate crystallites even in the miscible blend. When D_c exceeds 30−40 mol %, the blends become immiscible. These results clearly show that the relevance of the crystallization in the miscible blends to the absolute values of crystallization rate of components and their difference (or ratio). The higher crystallization rates and the smaller difference are advantageous to the cocrystallization.

In this paper, we try to separate the contributions of these two factors by the comparison of the phase structures among the five miscible blends of PHBV and PHBP. These pairs were selected so as to make variations in the crystallization rates of PHBV and PHBP

† The University of Tokyo.
‡ Tokyo Institute of Technology.
* Corresponding author. E-mail: yoshie@iis.u-tokyo.ac.jp.

10.1021/ma049858p CCC: $27.50
Published on Web 04/22/2004

and their ratio. Only PHBV and PHBP containing less than 20 mol % of HV or HP are used. In case that the HB unit is a major comonomer unit, both PHBV and PHBP crystallize in almost the same crystalline lattice as PHB homopolymer. A bit of difference in the lattice is that the *a* parameter of the crystalline unit cell slightly increases with the HV content for PHBV while no expansion occurs in the lattice of PHBP. Therefore, we can expect the occurrence of cocrystallization in some of the PHBV/PHBP blends under certain crystallization conditions.

The expansion in the crystalline lattice of PHBV is caused by isomorphism, i.e., the partial inclusion of HV units into the PHB crystalline lattice.[19−24] Isomorphism was not observed in PHBP. With the aid of this slight difference, we try to understand the role of the blend component inducing the cocrystallization, i.e., the component with the faster crystallization rate, systematically. Through the comparison between the blend of PHBV with faster crystallization rate and PHBP with slower crystallization rate and the blend of inverse combination, we will reveal the effect of the compatibility on the monomers in the crystalline lattice in the cocrystallization.

We analyze the phase structure of the blends through the in situ observation of the crystallization process by using FTIR microscope and the measurement of melting curve by DSC. To trace the crystallization process of the blend components separately by a FTIR microscope, deuterated PHBV (D-PHBV) is blended with normal PHBP. The C−D and C═O stretching bands of the IR spectra are used to trace the crystallization of D-PHBV and the whole blend, respectively.

Experimental Section

Materials. PHBV and PHBP samples were prepared by fermentation of *Ralstonia eutropha* H16 (ATCC17699) and *Alcaligenes latus* (ATCC 29713), respectively, as previously reported.[25,26] Carbon sources used for the biosynthesis of PHBV and PHBP are a mixture of acetic and propionic acids and a mixture of (*R*)-3-hydroxybutyric and 3-hydroxypropionic acids, respectively. For the biosynthesis of D-PHBV, perdeuterated acids were used. After extraction from the dried cells with hot chloroform, the copolyesters were compositionally fractionated by using chloroform/heptane mixed solvent, as previously reported.[27,28] PHBV containing 10 mol % HV [PHBV10], D-PHBV containing 6, 8, and 19 mol % HV [D-PHBV6, D-PHBV8, and D-PHBV19], and PHBP containing 11 and 15 mol % HP [PHBP11 and PHBP15] were used in this study.

It has been known that even if perdeuterated carbon source is used for the biosynthesis, only partially deuterated polyesters are produced due to the substitution of ^{2}H with ^{1}H during the metabolic process of the polyester synthesis.[29,30] The ^{2}H content of D-PHBV was determined by ^{1}H and ^{2}H NMR spectroscopy as previously reported.[29] For all the D-PHBV samples, the ^{2}H contents in main-chain methine, main-chain methylene, and side-chain groups were within the range of 0.25 ± 0.05, 0.65 ± 0.05, and 0.75 ± 0.05, respectively, which give the average ^{2}H content as 0.65 ± 0.05. This range of ^{2}H content is enough for the observation of the C−D bands by a FTIR microscope.

Some molecular characteristics of the copolyester samples are listed in Table 1. Molecular weight characterization was performed by a gel-permeation chromatograph (GPC) equipped with a refractive detector. Polystyrene standards with low polydispersity were used to construct a calibration curve. The comonomer composition was determined by ^{1}H NMR spectroscopy. For D-PHBV, the HV content was also determined by ^{2}H NMR spectroscopy. The values obtained from the ^{1}H and ^{2}H spectra agree within a range of experimental error. This indicates the similarity between the ^{2}H contents of HV and HB units. Only the composition determined by ^{1}H NMR spectroscopy is shown in Table 1.

Table 1. Molecular Characteristics of PHBV and PHBP

polyester	comonomer content/mol % [a]	$M_w \times 10^{-5}$ [b]	M_w/M_n [b]
D-PHBV6	5.9	14.6	1.8
D-PHBV8	8.0	14.8	1.8
PHBV10	10.0	12.1	2.2
D-PHBV19	18.7	17.1	1.8
PHBP11	11.1	3.2	1.8
PHBP15	15.2	4.9	1.7

[a] HV content for PHBV and HP content for PHBP. Measured by ^{1}H NMR. [b] Measured by GPC.

Blending of PHBV and PHBP was performed by a conventional solvent-casting technique from chloroform solution using a glass Petri dish as a cast surface. The crystallization behavior of the 1/1 blends along with their pure components was analyzed.

FT-IR Microscopy. Crystallization of samples was observed in situ with a Shimadzu AIM-8800 FTIR microscope equipped with a Mettler FP82HT hot stage. A cast film sample was heated to 195 °C, kept for 2 min, and then quickly cooled to a predetermined crystallization temperature, T_c, where it was kept isothermally. A growing spherulite residing apart from the others was found under polarized microscopic mode of the FTIR microscope. A square aperture (30×30 μm) for the measurement of FTIR spectra was set in parallel with and apart from the growing front of the spherulite. The spherulites of D-PHBV and PHBP grow to a few hundred micrometers in diameter at the crystallization conditions used in this study. A FTIR microscope allows us to observe the crystallization inside a spherulite. A series of FTIR spectra were recorded with a resolution of 4 cm^{-1} at specified time intervals. The measurements were started well before the growing front of the spherulite went into the aperture and continued until long after the front left the aperture area. The crystallization of samples was traced by the change of the C═O and C−D stretching bands at 1722 and 2230 cm^{-1}, respectively. Because of the large difference in the molar absorbance coefficients, the C═O and C−D stretching bands were measured separately. A thick film sample on a BaF_2 plate was used for the C−D band observation, while a thin sample inserted between the BaF_2 plates was used for the observation of the C═O band.

Measurement of Isothermal Spherulite Growth Rate. The isothermal spherulite growth rate, *G*, of samples was measured with an Olympus BX90 polarizing optical microscope equipped with a Mettler FP82HT hot stage. A film sample was heated to 195 °C, kept for 2 min, and then quickly cooled to a predetermined T_c where it was kept isothermally to observe spherulite growth. The *G* value was taken as the slope of the linear plot of spherulite radius vs time.

Observation of Melting Behavior by DSC. For the observation of melting behavior by DSC, isothermally crystallized samples were prepared by compression molding. A cast-film sample was inserted between aluminum plates with an aluminum spacer (0.1 mm thickness) and was compression-molded at 195 °C for 3 min under a pressure of 5 MPa by using a Toyoseiki Mini Test Press-10. The molten sample was then cooled to a predetermined T_c and kept for 4 weeks to reach the equilibrium crystallinity. Thermal analysis was carried out by a SEIKO EXSTAR6000 system equipped with a DSC 220U. The isothermally crystallized sample of 2−3 mg in aluminum pans was heated from −80 to 200 °C at a heating rate of 10 °C/min. The melting temperature, T_m, was taken as the peak top of the DSC endotherm.

Results and Discussion

Blend samples were prepared for the five pairs of PHBV and PHBP. They are (i) D-PHBV8/PHBP11, (ii) D-PHBV6/PHBP11, (iii) PHBV10/PHBP15, (iv) PHBP15/D-PHBV19, and (v) PHBP11/D-PHBV19. These pairs were selected so as to make variations in the *G* values

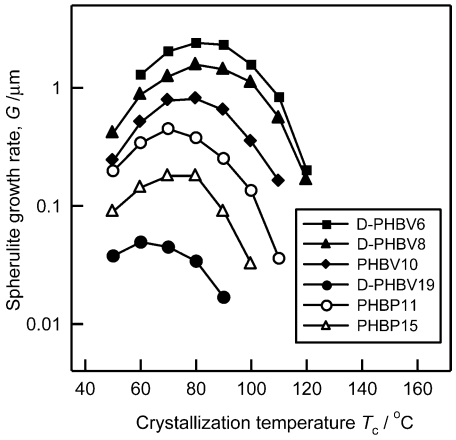

Figure 1. Variation in *G* with the crystallization temperature of PHBV and PHBP.

and their ratio of blend components. Figure 1 shows *G* of PHBV and PHBP as a function of T_c. The *G* value decreases with the increase of the content of the secondary comonomer (HV or HP). In the blend notation A/B, the component A has higher *G* than the component B. PHBV has a higher *G* than PHBP in blends (i)−(iii), while PHBP has a higher one in blends (iv) and (v). The *G* ratio of component A to component B for the blends is summarized in Table 2.

Miscibility in the Melt. First, the miscibility in the amorphous phase of the blends of PHBV and PHBP was analyzed through the observation of spherulite growth by a polarized optical microscope. The observation was performed for each sample at various temperatures between 50 and 120 °C. For all the blend samples at every temperature, no phase separation was observed visually, and spherulites grow linearly with time. Parts a−e of Figure 2 show *G* of the five blends as a function of T_c. *G* values of the pure components are also plotted. These figures clearly show that the *G* value of the blends is in between the *G* values of the pure components. These results indicate the miscibility between PHBV and PHBP in these blends.

As mentioned above, the blends of two PHBV or two PHBP with different comonomer compositions are miscible when the difference in the comonomer composition is small while the blend becomes immiscible when the difference exceeds 30−40 mol %.[9,11,13,16−18] This fact strongly suggests that the miscibility of the blends of PHBV and PHBP also depends on the HV and HP contents of the component copolymers. Though all the blends studied here are miscible, the blends of PHBV and PHBP with larger comonomer contents may become immiscible.

Crystallization in Blend (i) D-PHBV8/PHBP11. The crystallization behavior of the blend was analyzed

Table 2. Ratio of Spherulite Growth Rates (*G*) of Components and Phase Structure of the 1/1 Blends of PHBV and PHBP at 80−100 °C

		G ratio of A to B			phase structure[a]		
blend	A/B	80 °C	90 °C	100 °C	80 °C	90 °C	100 °C
(i)	D-PHBV8/PHBP11	4.2	5.7	8.3	(1)	(2)	(2)
(ii)	D-PHBV6/PHBP11	6.4	9.2	11.7	(1)	(3)	(4)
(iii)	PHBV10/PHBP15	4.5	7.2	10.8	(1)	(4)	n.d.[b]
(iv)	PHBP15/D-PHBV19	5.3	5.3	n.d.[b]	(1)	(1)	n.d.[b]
(v)	PHBP11/D-PHBV19	11.1	14.9	n.d.[b]	(1)	(1)	n.d.[b]

[a] (1) = complete cocrystallization, (2) = formation of cocrystals rich in component A, (3) = phase segregation forming crystals rich in component A and microcrystals of component B, (4) = phase segregation forming crystals of component A and microcrystals of component B. The degree of phase segregation increases as (1) < (2) < (3) < (4). The schematic representations of the phase structures are given in Figure 7. [b] Data not determined.

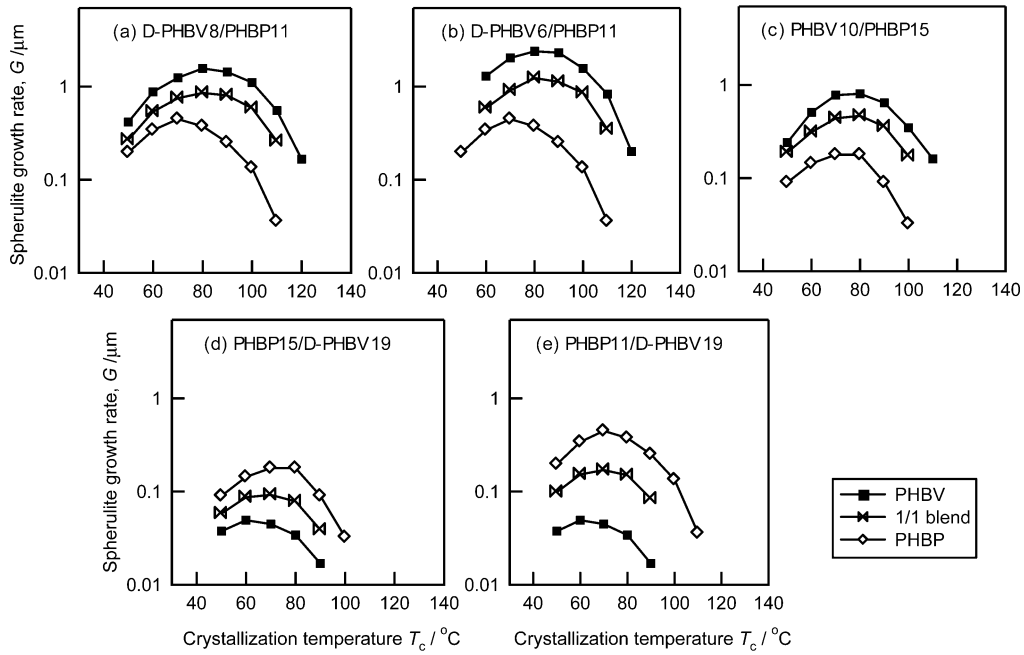

Figure 2. Variation in *G* with the crystallization temperature for 1/0, 1/1, and 0/1 blends of (a) D-PHBV8/PHBP11, (b) D-PHBV6/PHBP11, (c) PHBV10/PHBP15, (d) PHBP15/D-PHBV19, and (e) PHBP11/D-PHBV19.

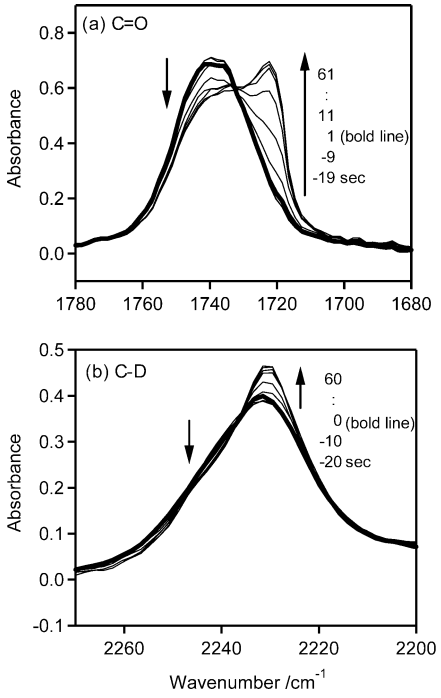

Figure 3. Time-resolved (a) C═O and (b) C−D stretching bands of FTIR spectra of D-PHBV8/PHBP11 during isothermal crystallization at 80 °C.

through the in situ observation by a FTIR microscope. Figure 3 shows the time-resolved C═O and C−D stretching bands of the FTIR spectra for the 1/1 D-PHBV8/PHBP11 blend during isothermal crystallization at 80 °C. Time t is set to be zero just when the growing front of a spherulite enters the aperture area. The C═O and C−D bands are approximately symmetrical before the entry of the growing front of the spherulite into the aperture area ($t < 0$) whereas additional peaks begin to appear at the lower wavenumber side of these bands when the growing front reaches this area ($t > 0$). These additional peaks must be ascribed to the crystalline phase.

The C═O and C−D stretching bands were used to analyze the crystallization behavior of the whole blend and of the D-PHBV component in the blend, respectively, by the procedure described in a previous paper.[12] In brief, these bands are analyzed with a simple two-peak model, in which each of the C═O and C−D bands is assumed to be comprised of a peak from the crystalline phase and one from the amorphous phase. In this model, the relative degree of crystallinity, $X(\nu,t)$ can be estimated from the C═O (ν = 1722 cm^{-1}) or C−D (ν = 2230 cm^{-1}) band as

$$X(\nu,t) = c(t)/c(\infty) = [A(\nu,t) - A(\nu,-\infty)]/[A(\nu,\infty) - A(\nu,-\infty)] \quad (1)$$

where $c(t)$ is the degree of the crystallinity at time t and $A(\nu,t)$ is the absorbance at time t and wavenumber ν. $A(\nu,-\infty)$ and $A(\nu,\infty)$ are the absorbances of the sample in the complete amorphous state and of the sample reaching its equilibrium crystallinity, respectively.

Figure 4 shows the time dependence of the relative crystallinity, $X(\nu,t)$, for D-PHBV8, PHBP11, and their 1/1 blend crystallized at 80−100 °C. For the pure D-PHBV8, the time dependence of $X(2230,t)$ completely accords with that of $X(1722,t)$, indicating that the changes in C═O and C−D bands reflect the same conformational change or the synchronizing conformational changes during the crystallization of D-PHBV8. Therefore, we can evaluate the difference in the crystal-

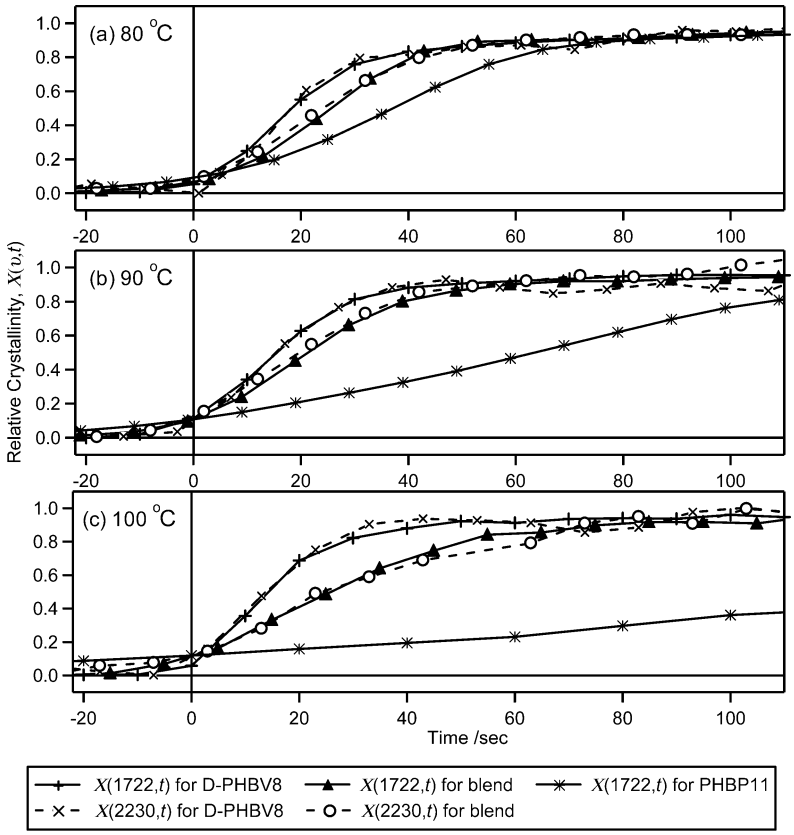

Figure 4. Time dependence of the relative crystallinity, $X(\nu,t)$, for D-PHBV8, PHBP11, and their 1/1 blend crystallized at (a) 80, (b) 90, and (c) 100 °C.

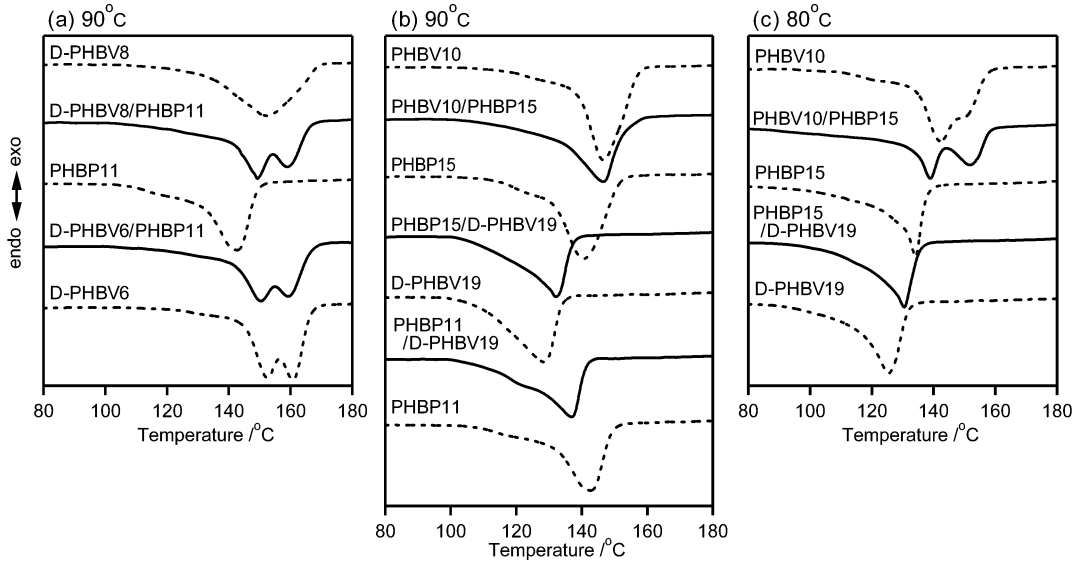

Figure 5. DSC melting curve of PHBV/PHBP blends and their components crystallized at (a, b) 90 and (c) 80 °C.

lization process of the components in D-PHBV/PHBP blends separately through the comparison of $X(1722,t)$ and $X(2230,t)$. $X(1722,t)$ reflects the crystallization behavior of the overall blends, while $X(2230,t)$ allows picking out the information on the D-PHBV component. It should be noted that the time dependence of $X(\nu,t)$ is characterized by a sigmoid curve, which begins to grow before the growing front of the spherulite enters the aperture area ($t < 0$) and continues to grow after the front exits the aperture ($t > t_{pass}$, t_{pass} is the time just when the front exits the aperture). Although the behavior at $t < 0$ may be partially ascribed to some kind of conformational change that happens before the formation of spherulite becomes visible, the main cause of it must be diffraction of IR light. When the growing front of the spherulite reaches just outside the aperture, part of the light diffracted by the aperture plates passes through the spherulite and skews the spectrum. Though light diffraction also contributes to the increase of $X(\nu,t)$ at $t > t_{pass}$, the larger increase of $X(\nu,t)$ at $t > t_{pass}$ in the longer period indicates the contribution of the secondary crystallization. Since the contribution of the diffraction cannot be separated from the spectra, only the difference between $X(1722,t)$ and $X(2230,t)$ is used to analyze the crystallization process in this study.

At 80−100 °C, $X(2230,t)$ and $X(1722,t)$ of the 1/1 D-PHBV8/PHBP11 blends completely accord with each other. This indicates the cocrystallization of D-PHBV8 and PHBP11 at these temperatures. It is reasonable to assume that the crystallization in this blend is induced by D-PHBV8, i.e., the component crystallizing faster in the pure state. The D-PHBV8 chains that are about to crystallize at the growing front of a spherulite trap the PHBP11 chains in the neighborhood and drag them into the growing front of the crystals. The fact that PHBP11 and D-PHBV8 in their pure states crystallize in almost the same PHB-type crystalline lattice at similar spherulite growth rates strongly suggests that the PHBP11 chains can form a conformation that matches up well with the crystalline lattice of D-PHBV8 at a rate similar to D-PHBV8. Therefore, PHBP11 can cocrystallize with D-PHBV8.

In that context, the existence of D-PHBV8 accelerates the crystallization of PHBP11. The existence of PHBP11, on the other hand, retards the crystallization of D-PHBV8 because the crystalline lattice of PHBP11 is not exactly the same as that of D-PHBV8. As a result, D-PHBV8 and PHBP11 cocrystallizes at a rate between the crystallization rates of pure D-PHBV8 and pure PHBP11. $X(1722,t)$ of this blend grows at just about the average rate of $X(1722,t)$s of pure D-PHBV8 and pure PHBP11 at 80 °C, while it grows faster than the average at 90 and 100 °C. As shown in a previous paper,[10,11] the composition dependence of G reflects the crystalline phase structure. The G value of a 1/1 blend showing complete cocrystallization approximately corresponds with the geometric mean of the G values of the blend components, while the G value of a 1/1 blend showing phase segregation is higher than this. The T_c dependence of the growing rate of $X(\nu,t)$ suggests that the PHBP11 content in the crystalline phase of the blend decreases as T_c increases. The crystalline phase formed at 80 °C is probably the complete cocrystals whose PHBP11 content is similar to the blend composition, while the crystalline phase formed at 90 and 100 °C is rich in D-PHBV8.

The upper three curves of Figure 5a shows the DSC melting cure of this blend and its components crystallized at 90 °C. Though the blend showed two-peak melting behavior, the higher temperature peak was ascribed to the melt/recrystallization process by means of repeated DSC measurements with various heating rates (data not shown). Only the lower temperature peak represents the melting of the crystals formed at 90 °C. The T_m values, i.e., the peak position of the lower temperature peak, of D-PHBV8, PHBP11, and their 1/1 blend are summarized in Table 3. The average of the melting temperatures of the pure components, D-PHBV8 and PHBP11, is also shown in this table. It has been known that, similar to the behavior of G, the composition dependence of T_m in two PHBV blends reflects the crystalline phase structure.[10−12] The T_m value of the 1/1 blend showing complete cocrystallization approximately corresponds with the arithmetic mean of the T_m values of the blend components, while the T_m value of the 1/1 blend showing phase segregation is higher than this. The T_m value of the D-PHBV8/PHBP11 blend is a little bit higher than the average of the pure components, which is consistent with the

Table 3. Melting Temperature of PHBV, PHBP, and Their 1/1 Blends Crystallized at 80 and 90 °C

			melting temp/°C			
blend	A/B	crystallization temp/°C	A	B	1/1 blend	av of A and B
(i)	D-PHBV8/PHBP11	90	152.4	142.6	149.3	147.5
(ii)	D-PHBV6/PHBP11	90	152.6	142.6	150.4	147.6
(iii)	PHBV10/PHBP15	80	142.2	134.1	138.8	138.2
(iii)	PHBV10/PHBP15	90	146.6	137.0	146.5	141.8
(iv)	PHBP15/D-PHBV19	80	134.1	125.4	130.4	129.8
(iv)	PHBP15/D-PHBV19	90	137.0	128.5	132.0	132.8
(v)	PHBP11/D-PHBV19	90	142.6	128.5	136.9	135.6

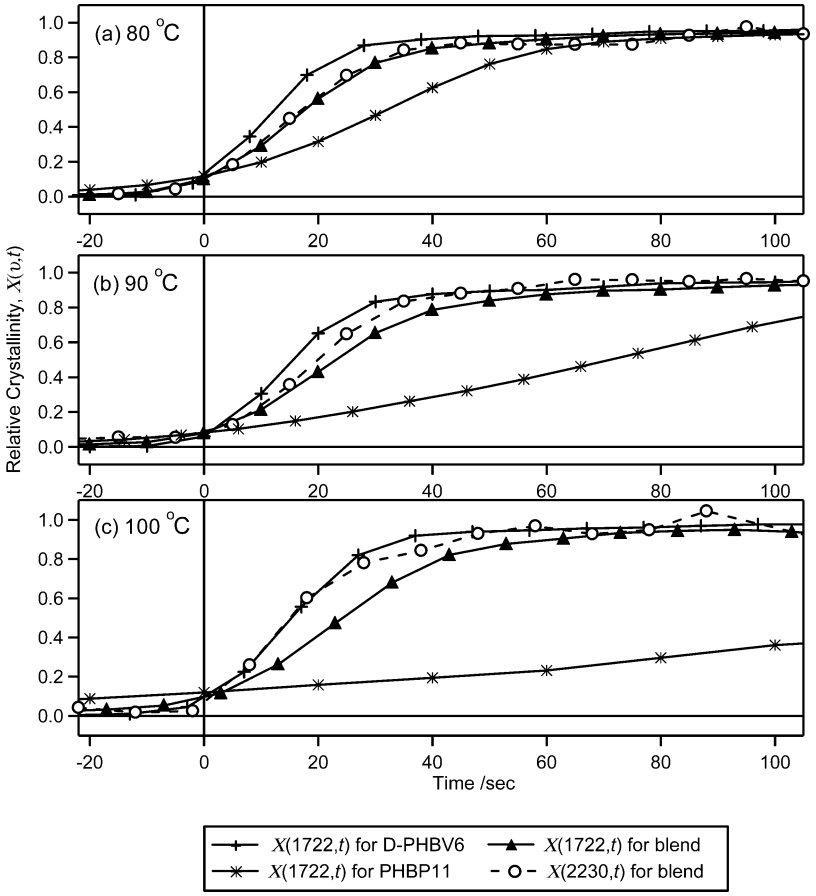

Figure 6. Time dependence of the relative crystallinity, $X(\nu,t)$, for D-PHBV6, PHBP11, and their 1/1 blend crystallized at (a) 80, (b) 90, and (c) 100 °C.

hypothesis of the formation of the D-PHBV8-rich crystals at 90 °C.

Crystallization in Blend (ii) D-PHBV6/PHBP11. The second blend is D-PHBV6/PHBP11, of which the PHBV component has a higher G than blend (i) (= D-PHBV8/PHBP11) and, as a result, of which the G ratio is larger than that of blend (i) (see Figure 1 and Table 2).

Figure 6 shows the time dependence of the relative crystallinity, $X(\nu,t)$, of D-PHBV6, PHBP11, and their 1/1 blend crystallized at 80−100 °C. Similar to the case of the pure D-PHBV8, $X(2230,t)$ completely accorded with $X(1722,t)$ for the pure PHBV6. The data of $X(2230,t)$ for the pure D-PHBV6 were omitted from Figure 6 for ease to read the data. At 80 °C, $X(2230,t)$ and $X(1722,t)$ of the 1/1 D-PHBV6/PHBP11 blend grow simultaneously, indicating that PHBP11 cocrystallizes with PHBV6. Since $X(1722,t)$ grows at approximately the average rate of $X(1722,t)$s of pure D-PHBV6 and pure PHBP11, the crystalline phase are probably the complete cocrystals whose PHBP11 content is similar to the blend composition.

On the other hand, $X(2230,t)$ grows a little bit faster than $X(1722,t)$ at 90 °C. This indicates that phase segregation occurs at the crystalline growing front at this temperature. The crystals rich in D-PHBV6 are formed first, which is followed by the crystallization of PHBP11. The formation of the D-PHBV6-rich crystals must be induced by D-PHBV6, i.e., the component crystallizing faster in the pure state. The D-PHBV6 chains that are about to crystallize trap the PHBP11 chains in the neighborhood and try to drag them into the crystalline phase. However, the PHBP11 chains have little time to adopt a conformation that matches up to the crystalline lattice of D-PHBV6 because the G value of D-PHBV6 is much higher than that of PHBP11. Therefore, most of the PHBP11 chains escape from the crystalline growth front. The fact that no phase segregation is observed by a polarized microscope shows that the PHBP11 chains are left between the D-PHBV6 lamellas and crystallize there later.

The melting behavior of this blend and its components crystallized at 90 °C was also observed by DSC (the lower three curves in Figure 5a). Thought this blend

and pure D-PHBV6 showed two-peak melting behavior, the higher temperature peak was ascribed to the melt/recrystallization process again. T_m of D-PHBV6, PHBP11, and their 1/1 blend are shown in Table 3. The T_m value of the blend is quite higher than the average of the components. This also supports the hypothesis that the preceding crystals contain only little amount of PHBP11. The fact that only one T_m was observed suggests the smallness of the crystals lately formed by PHBP11. Because of the limitation in space, PHBP11 can form only microcrystals of which heat of fusion is too small to be detected by DSC.

At 100 °C, the difference between $X(2230,t)$ and $X(1722,t)$ becomes larger, and $X(2230,t)$ of the blend agrees with that of the pure PHBV6. Therefore, PHBP11 must be completely excluded from the preceding crystals. The resulting phase structure is composed of the crystals of pure D-PHBV6 and microcrystals of PHBP11.

The phase structures of the blends (i) D-PHBV8/PHBP11 and (ii) D-PHBV6/PHBV11 are summarized in Table 2. Blend (ii) forms two separated crystalline phases above 90 °C, while blend (i) still forms only one cocrystalline phase at 90 and 100 °C. The G value of D-PHBV6 is larger than that of D-PHBV8, which results in the larger G ratio for blend (ii). It has been shown that larger G value is advantageous for the cocrystallization, while a larger G ratio is disadvantageous for it.[10,11] In the case of blends (i) and (ii), the phase structure is more sensitive to the latter effect than the former. Since the G ratios of blend (ii) at 100 °C (at which the blend has only one cocrystalline phase) and of blend (i) at 90 °C (at which the blend shows two separated crystalline phases) are 8.3 and 9.2, respectively, the threshold of separation in the G ratio seems to be around 9. For different pair of PHBV/PHBP, however, the absolute G values may also influence the phase structure. To consider this effect, the blend (iii) PHBV10/PHBP15 is analyzed.

Melting Behavior of Blend (iii) PHBV10/PHBP15. The G values of the components of this blend is lower than those of blends (i) and (ii), while the G ratio is between them (see Figure 1 and Table 2).

Because PHBV10 is not deuterated, FTIR microscopy has no use for the analysis of phase segregation of this blend. The phase structure was only analyzed through the observation of the melting behavior by DSC measurements. The DSC melting curves of the 1/1 PHBV10/PHBP15 blend and its components crystallized at 80 and 90 °C are shown in the upper part of Figure 5, b and c, respectively. Though some of the samples show two-peak melting behavior, it was ascribed to the melt/recrystallization process again. The T_m values are summarized in Table 3.

The T_m value of the blend crystallized at 80 °C corresponds to the average of the pure components, indicating the formation of complete cocrystals. On the other hand, the T_m value of the blend crystallized at 90 °C is almost the same as that of PHBV10, suggesting that the crystals are composed of only PHBV10. As mentioned above, melting peak of the microcrystals in blend (ii) was not observed on the DSC melting curve. This implies that the formation of microcrystals in the 1/1 PHBV10/PHBP15 blend at 90 °C cannot be judged by DSC analysis. It would not be expected that PHBP15 that accounts for 50% of the blend stays in amorphous phase at 90 °C for the time as long as 4 weeks (= crystallization period used in this study). Therefore, PHBP15 probably forms microcrystals.

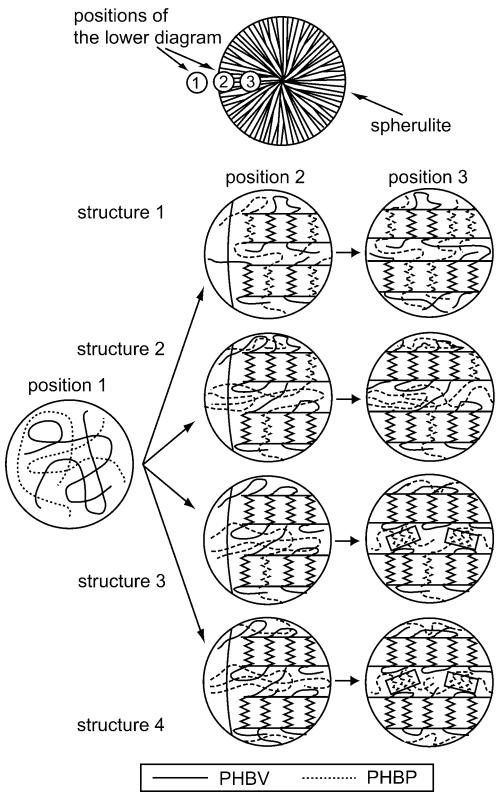

Figure 7. Schematic diagram illustrating the crystallization process in the PHBV/PHBP blends. Positions 1, 2, and 3 indicate the outside of spherulites, the position just on the growing line of a spherulite, and the inside of the spherulite as illustrated in the upper diagram.

The phase structure of the PHBV10/PHBP15 blend is also summarized in Table 2. Although the G ratio is smaller than 9, PHBV10/PHBP15 probably forms separate crystals of PHBV10 and microcrystals of PHBP15 at 90 °C. This indicates the effect of the absolute G value on the phase structure of the PHBV/PHBP blends. Despite the ultimate resemblance of the crystalline lattice between PHBV and PHBP, the PHBP chains are just the lattice defects in the PHBV crystals. The PHBP chains escape from the growing front of the PHBV crystals if possible. The glass transition temperatures of all the PHBV and PHBP components of blends (i)−(iii) are within the range of 2 ± 3 °C, indicating that these copolymers have similar molecular mobility at 90 °C. In such a case, the smaller G value of PHBV gives the PHBP chains longer time to escape from the crystalline growing front.

Crystalline Phase Structure of the PHBV/PHBP Blend. As summarized in Table 2, the PHBV/PHBP blends form various crystalline phase structures depending on the comonomer compositions of PHBV and PHBP and the crystallization temperature. The phase structures are (1) complete cocrystallization, (2) formation of PHBV-rich cocrystals, (3) phase segregation forming PHBV-rich cocrystals and PHBP microcrystals, and (4) phase segregation forming PHBV crystals and PHBP microcrystals. In these phase structures, the extent of phase segregation upon the crystallization increases in this order. Two of the determinant factors of the extent of phase segregation are the G value of PHBV and the G ratio of PHBV to PHBP. Figure 7 shows a schematic diagram illustrating the crystalliza-

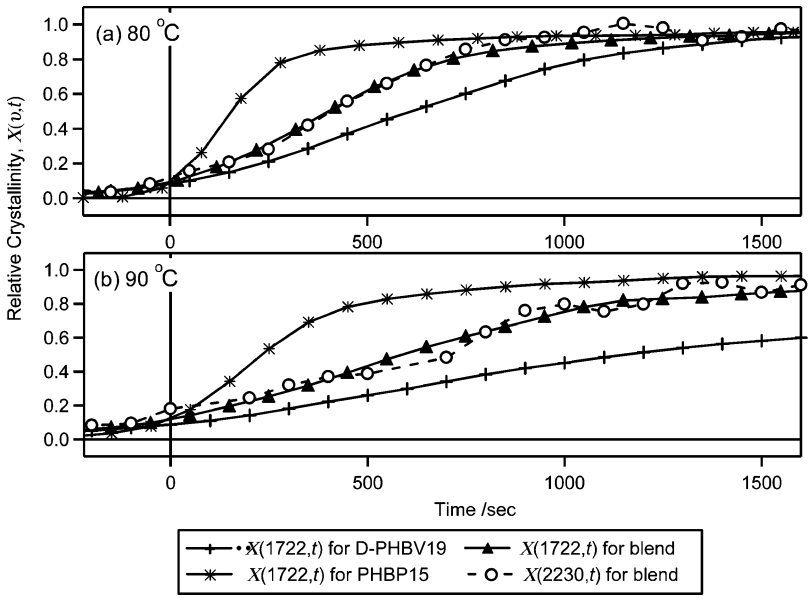

Figure 8. Time dependence of the relative crystallinity, $X(v,t)$, for PHBP15, D-PHBV19, and their 1/1 blend crystallized at (a) 80 and (b) 90 °C.

tion process in the PHBV/PHBP blends. When the *G* value of PHBV is high and the *G* ratio is small, PHBV and PHBP cocrystallize as if they are the same polymers [phase structure (1)]. The composition in the crystalline phase is the same as the blend composition. When the *G* value of PHBV become lower and/or the *G* ratio become larger, the phase segregation proceeds to form the crystalline phase rich in PHBV. When the PHBP content in the PHBV-rich crystalline phase is still not small, the crystallization event of the blend is finished up with the formation of this phase [phase structure (2)]. When the phase segregation proceeds further and PHBP content in the PHBV-rich crystals becomes very small, a substantial amount of PHBP and small amount of PHBV remain in the amorphous phase, which form the separated microcrystals of PHBP (and PHBV) later [phase structure (3)]. If the phase segregation occurs completely, the crystalline phase of pure PHBV and the microcrystals of PHBP are formed [phase structure (4)].

Crystallization in Blend (iv) PHBP15/D-PHBV19. The *G* ratio of this blend is almost the same as blend (iii) while the absolute *G* values are smaller. It should be noted that, opposite to blends (i)−(iii), the *G* value of PHBP is larger than that of PHBV in this blend.

Figure 8 shows the time dependence of $X(v,t)$ of PHBP15, D-PHBV19 and their 1/1 blend at 80 and 90 °C. At these temperatures, $X(2230,t)$ and $X(1722,t)$ of the blend grow simultaneously, indicating that D-PHBV19 cocrystallizes with PHBP15. Since $X(1722,t)$ grows at approximately the average rate of $X(1722,t)$s of pure PHBP15 and pure D-PHBV19, the crystalline phase are probably the complete cocrystals. The DSC melting curves of PHBP15, D-PHBP19, and their 1/1 blend crystallized at 80 and 90 °C are shown in parts b and c of Figure 5, respectively. The T_m values determined by DSC are summarized in Table 3. The T_m value of the blend corresponds to the average of the components, supporting the hypothesis of the formation of complete cocrystals. This is contrary to the results of PHBV/PHBP blends, where a smaller *G* value is disadvantageous for the cocrystallization. This might be relevant to the reversal of the magnitude relation of *G* between PHBV and PHBP. This possibility is further discussed with the data of blend (v) in the next section.

Crystallization in (v) PHBP11/D-PHBV19. The last blend is PHBP11/D-PHBV19. This blend is comprised of the components with the lowest *G* value and the largest *G* ratio. Figure 9 shows the time dependence of $X(v,t)$ for PHBP11, D-PHBV19 and their 1/1 blend at 80 and 90 °C. At these temperatures, $X(2230,t)$ and $X(1722,t)$ for the blend again grow simultaneously, indicating that D-PHBV19 cocrystallizes with PHBP11. Since $X(1722,t)$ grows at approximately the average rate of $X(1722,t)$s of pure PHBP11 and pure D-PHBV19, the crystalline phase are probably the complete cocrystals. The DSC melting curves of PHBP11, D-PHBP19, and their 1/1 blend crystallized at 90 °C are shown in Figure 5b. The T_m values are summarized in Table 3. The T_m value of the blend crystallized at 90 °C corresponds to the average of the components, supporting the hypothesis of the formation of complete cocrystals.

Despite the lowest *G* value and the largest *G* ratio, the extent of phase segregation in this blend is lower than PHB10/PHBP15 and D-PHBV6/PHBP11 at 90 °C. The result also supports the relevance of the capacity for cocrystallization to the magnitude relation of *G* between PHBV and PHBP.

Difference in Crystalline Phase Structure between PHBV/PHBP and PHBP/PHBV. The difference in the capacity for cocrystallization between PHBV/PHBP and PHBP/PHBV is probably related to the difference in the compatibility of HV and HP units to the PHB crystalline lattice. One of the dominant characteristics of PHBV is isomorphous behavior; i.e., HV units are included into the PHB lattice and vice versa in the PHV lattice.[19−24] The coexistence of HB and HV units in a crystalline lattice results in high crystallinity and thick lamellas even at the intermediate comonomer composition.[31] In the case of PHBV containing less than 20% HV crystallized at 80−100 °C, the crystallinity exceeds 50% and the lamella thickness is 5−7 nm,[32,33] which are comparable to the values of the PHB homopolymer. On the other hand, the PHB copolymers other than PHBV do not show isomorphous behavior.[34] As a result of the exclusion of comonomer units from

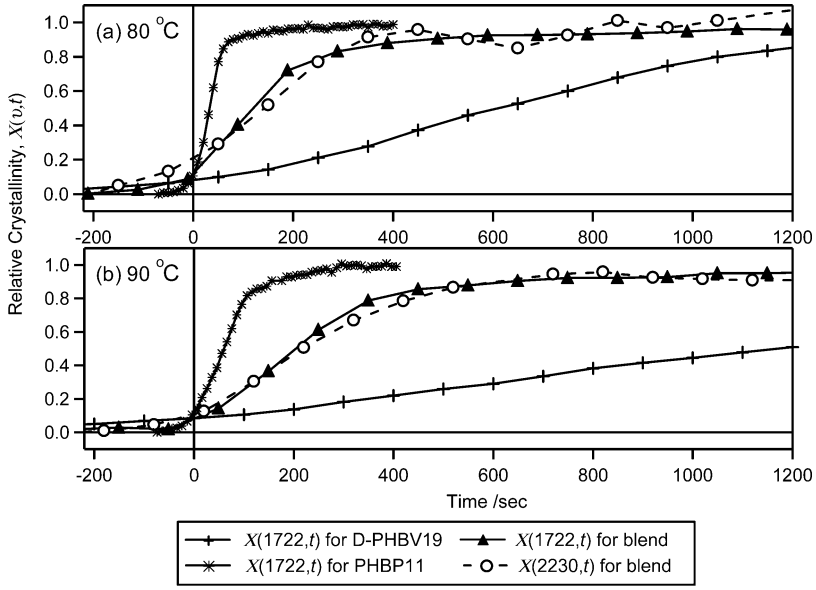

Figure 9. Time dependence of the relative crystallinity, $X(\nu,t)$, for PHBP11, D-PHBV19, and their 1/1 blend crystallized at (a) 80 and (b) 90 °C.

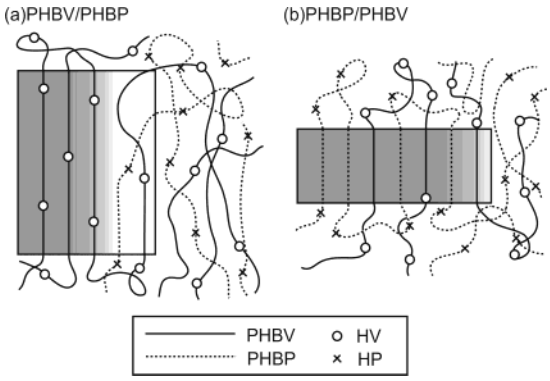

Figure 10. Schematic diagram illustrating the difference in the crystallization process between PHBV/PHBP and PHBP/PHBV blends.

the crystalline phase, the crystallinity and lamellar thickness of these copolymers rapidly decrease with the increase of comonomer content. In the case of PHBP, the copolymer becomes fully amorphous when the HP content becomes nearly 50%. Though there are no reports on the lamellar thickness of PHBP in our knowledge, the thickness of various PHB copolymers showing no isomorphism have been reported,[33] and all the copolymers have similar values. When the comonomer content is 5−10 mol %, the lamellas formed at 80−100 °C have thickness of 2−3 nm. The lamella thickness of PHBP is probably within this range. Therefore, in the pure state, PHBP forms lamellas much thinner than PHBV.

Figure 10 shows a schematic diagram illustrating the difference in the crystallization process between PHBV/PHBP and PHBP/PHBV blends. The crystallization in the blends of PHBV and PHBP is induced by the component having higher *G*. In PHBP/PHBV blends, PHBP leads the formation of relatively thin lamellas. Any part of PHBV chains easily gets into these lamellas because the HV units in the chains can participate in the PHB-type crystalline lattice. Therefore, PHBV easily cocrystallizes with PHBP in PHBP/PHBV blends. In PHBV/PHBP blends, on the other hand, PHBV leads relatively thick lamellas. Since the HP units in the PHBP chains cannot participate to the PHB-type lattice, only the homogeneous sequences of HB units longer than the lamellas can participate to the lamellas induced by PHBV. Thus, PHBP hardly cocrystallizes with PHBV in PHBV/PHBP blends. In this manner, the difference in the compatibility of HV and HP units to the PHB crystalline lattice affects the crystallization of the blends of PHBV and PHBP.

Conclusions

As shown in Table 2, the blends of PHBV and PHBP adopt various phase structures. The comparison of the crystalline phase structure among PHBV/PHBP blends indicates the significance of the *G* values and their ratio of the blend components on the crystallization process. The extent of phase segregation upon the crystallization in these blends increases with the decrease of the *G* value and with the increase of the *G* ratio.

The comparison of PHBV/PHBP blends with PHBP/PHBV blends indicates another important factor for cocrystallization. In PHBV/PHBP blends, PHBP is hardly able to participate in the thick lamellas induced by PHBV because the HP units that are randomly distributed in the PHBP chain are excluded from the crystalline lattice. In PHBP/PHBV blends, on the other hand, PHBV can easily participate to the lamellas induced by PHBP due to the isomorphous behavior. Accordingly, the compatibility of the chains of the component with lower *G* to the crystalline lattice of the other component affects the extent of cocrystallization.

References and Notes

(1) Alamo, R. G.; Glaser, R. G.; Mandelkern, L. *J. Polym. Sci., Part B: Polym. Phys.* **1988**, *26*, 2169.

(2) Tashiro, K.; Imanishi, K.; Izuchi, M.; Kobayashi, K.; Itoh, Y.; Imai, M.; Yamagichi, Y.; Ohashi, M.; Stein, R. S. *Macromolecules* **1995**, *28*, 8484 and references therein.

(3) Tanaka, H.; Lovinger, A. J.; Davis, D. D. *J. Polym. Sci., Part B: Polym. Phys.* **1990**, *28*, 2183.

(4) Runt, J.; Jin, L.; Talibuddin, S.; Davis, C. R. *Macromolecules* **1995**, *28*, 2781.

(5) Datta, J.; Nandi, A. K. *Polymer* **1998**, *39*, 1921 and references therein.

(6) Harris, J. E.; Robeson, L. M. *J. Polym. Sci., Part B: Polym. Phys.* **1987**, *25*, 311.
(7) Sham, C. K.; Guerra, G.; Karasz, F. E.; MacKnight, W. J. *Polymer* **1988**, *29*, 1016.
(8) Pal, S.; Nandi, A. K. *Macromolecules* **2003**, *36*, 8426.
(9) Yoshie, N.; Menju, H.; Sato, H.; Inoue, Y. *Polym. J.* **1996**, *28*, 45.
(10) Yoshie, N.; Fujiwara, M.; Ohmori, M.; Inoue, Y. *Polymer* **2001**, *42*, 8557.
(11) Saito, M.; Inoue, Y.; Yoshie, N. *Polymer* **2001**, *42*, 5573.
(12) Yoshie, N.; Asaka, A.; Yazawa, K.; Kuroda, Y.; Inoue, Y. *Polymer* **2003**, *44*, 7405.
(13) Na, Y. H.; Arai, Y.; Asakawa, N.; Yoshie, N.; Inoue, Y. *Macromolecules* **2001**, *34*, 4834.
(14) Doi, Y. *Microbial Polyesters*; VCH Publishers: New York, 1990.
(15) *Biopolymers*; Doi, Y., Steinbüchel, A., Eds.; John Wiley & Sons: New York, 2001; Vols. 3, 3b, and 4.
(16) Organ, S. J.; Barham, P. J. *Polymer* **1993**, *34*, 2169.
(17) Organ, S. J. *Polymer* **1994**, *35*, 86.
(18) Pearce, R. P.; Marchessault, R. H. *Macromolecules* **1994**, *27*, 3869.
(19) Bluhm, T. L.; Hamer, G. K.; Marchessault, R. H.; Fyfe, C. A.; Veregin, R. P. *Macromolecules* **1986**, *19*, 2871.
(20) Barker, P. A.; Mason, F.; Barham, P. J. *J. Mater. Sci.* **1990**, *25*, 1952.
(21) Kamiya, N.; Sakurai, M.; Inoue, Y.; Chûjô, R.; Doi, Y. *Macromolecules* **1991**, *24*, 2178.
(22) Kamiya, N.; Sakurai, M.; Inoue, Y.; Chûjô, R. *Macromolecules* **1991**, *24*, 3888.
(23) Yoshie, N.; Sakurai, M.; Inoue, Y.; Chûjô, R. *Macromolecules* **1992**, *25*, 2046.
(24) Sánchez-Cuesta, M.; Martínez-Salazar, J.; Barker, P. A.; Barham, P. J. *J. Mater. Sci.* **1992**, *27*, 5335.
(25) Doi, Y.; Kunioka, M.; Nakamura, Y.; Soga, K. *Macromolecules* **1987**, *20*, 2988.
(26) Hiramitsu, M.; Doi, Y. *Polymer* **1993**, *34*, 4782.
(27) Yoshie, N.; Menju, H.; Sato, H.; Inoue, Y. *Macromolecules* **1995**, *28*, 6516.
(28) Cao, A.; Kasuya, K.; Abe, H.; Doi, Y.; Inoue, Y. *Polymer* **1998**, *39*, 4801.
(29) Yoshie, N.; Goto, Y.; Sakurai, M.; Inoue, Y.; Chûjô, R.; Doi, Y. *Int. J. Biol. Macromol.* **1992**, *14*, 81.
(30) Gross, R. A.; Ulmer, H. W.; Lenz, R. W.; Tshudy, D. J.; Uden. P. C.; Brandt, H.; Fuller, R. C. *Int. J. Biol. Macromol.* **1992**, *14*, 33.
(31) Kunioka, M.; Tamaki, A.; Doi, Y. *Macromolecules* **1989**, *22*, 694.
(32) Yoshie, N.; Saito, M.; Inoue, Y. *Macromolecules* **2001**, *34*, 8953.
(33) Abe, H.; Doi, Y.; Aoki, H.; Akehata, T. *Macromolecules* **1998**, *31*, 1791.
(34) Cao, A.; Asakawa, N.; Yoshie, N.; Inoue, Y. *Polymer* **1999**, *40*, 3309.

MA049858P